Epilepsy Research 156 (2019) 106167

Contents lists available at ScienceDirect

Epilepsy Research

journal homepage: www.elsevier.com/locate/epilepsyres

The anticonvulsant and neuroprotective effects of kir2.3 activation in PTZ-induced seizures and the kainic acid model of TLE

Lu Zhang[a,1], Wanbing Sun[a,1], Lan Xu[a], Yue Wang[a], Guoxing Zhu[a], Xunyi Wu[a,*], Yun Wang[b,*], Zhen Hong[a]

[a] Department of Neurology at Huashan Hospital, Fudan University, Shanghai 200032, China
[b] Institutes of Brain Science, Department of Neurology at Zhongshan Hospital, Fudan University, Shanghai 200032, China

ARTICLE INFO

Keywords:
Kir2.3 channel
Tenidap
Pentylenetetrazol
Kainic acid
Seizure
Temporal lobe epilepsy

ABSTRACT

Purpose: To elucidate the role of activating the inwardly rectifying K^+ channel 2.3 (Kir2.3) in acute seizure and chronic epilepsy, we investigated the effect of a Kir2.3 agonist (tenidap) on epileptic and electrophysiological activities in mice. Neuronal excitability and damage were also evaluated.

Methods: A Pentylenetetrazole (PTZ)-induced acute seizure model and a kainic acid (KA)-induced temporal epilepsy model were used in adult mice. The mice were given tenidap 30 min before PTZ injection or were given tenidap for 7 days after entering the chronic stage of the KA model. Video monitoring and EEG recordings were performed for comparisons. Immunofluorescence of c-fos was detected in the PTZ model, and Nissl staining was performed in the KA model.

Results: Tenidap intervention significantly reduced the duration and severity of PTZ-induced acute seizures, which conformed with the power-spectrum analyses of the EEG and the quantification of spikes on EEG. C-fos expression representing neuronal excitability was also reduced with tenidap pretreatment. However, the latency time to seizure onset was unaltered. Seven days of tenidap treatment in the chronic KA model significantly attenuated seizure and spike frequencies compared to the same animal before administration. Nissl staining showed reduced hilar neuron loss in the tenidap-intervention group but showed no difference in the width of the granule cell layer.

Conclusion: To our knowledge, few studies have reported the relevance of Kir2.3 to epilepsy. The present data suggested that activation of Kir2.3 exerts an anticonvulsant effect in acute seizures and the chronic stage of TLE, which makes this channel a potent therapeutic target.

1. Introduction

Epilepsy is a common neurological disorder that is characterized by recurrent seizures resulting from abnormal synchronous neuronal activities involving ion channel dysfunction (Kambli et al., 2017). Various antiepileptic drugs (AEDs) exert their anticonvulsant effects by the modification of ion channel activities, including voltage-gated sodium and calcium channels (Rogawski and Loscher, 2004). Voltage-gated potassium channels, such as the Kv7 family, have also been reported to play an important role in the regulation of excitability in the brain, which is closely related to antiepileptic effects (Gunthorpe et al., 2012; Greene and Hoshi, 2017). However, the role of another family of potassium channels, the inwardly rectifying K^+ (Kir) channels, in inhibiting seizures is poorly understood (Neusch et al., 2003).

Kir channels are categorized into seven subfamilies (Kir1.0- Kir7.0). These channels mediate inward currents more readily and are activated near the resting potential (Hibino et al., 2010). Kir2.0 channels are widely distributed in various types of neural cells and play a prominent role in membrane potential hyperpolarization and neuronal excitability modulation of neurons. Glial Kir2.0 channels also buffer the concentration of extracellular potassium and maintain ion homeostasis (Neusch et al., 2003). Accumulating evidence shows that Kir2.0 channels may be associated with epilepsy. In the kainic acid (KA)-induced mouse model of temporal lobe epilepsy (TLE), Kir currents with classic Kir2 channel characteristics are significantly increased in epileptic granule cells of brain slices. The protein expression of Kir2.1-Kir2.4 subunits is also augmented in the acute phase (Young et al., 2009). Another functional study using patch-clamp techniques also suggested

* Corresponding authors.
E-mail addresses: dr.xunyiwu@163.com (X. Wu), wangyun1106@163.com (Y. Wang).
[1] These authors made equal contribution in this work.

https://doi.org/10.1016/j.eplepsyres.2019.106167
Received 6 February 2019; Received in revised form 6 July 2019; Accepted 12 July 2019
Available online 15 July 2019
0920-1211/

that compromised potassium buffering in the sclerotic hippocampus of TLE patients was attributed to impaired Kir channels (Das et al., 2012). However, which subunit is primarily responsible in TLE remains unknown.

In our previous study, we have revealed a bimodal expression pattern of Kir2.3 mRNA and protein in rat pilocarpine model. Both molecules increased 24 h post-status epilepticus (SE) and declined in the chronic stage when compared with the control group (Xu et al., 2013), which may indicate a relation between dysfunction of the Kir2.3 and TLE. However, the specific role of Kir2.3 must be confirmed systematically using EEG and epileptic behavior assays and tested in a chronic stage that is reminiscent of the clinical condition. With the help of a specific agonist of Kir2.3 channels named tenidap (Liu et al., 2002), we verified the anticonvulsant property of Kir2.3 activation in acute seizures and the disease-modifying effects during chronic stages of a TLE model in our present study. Furthermore, channel activation also impeded neuronal excitability and cytoarchitectural alterations associated with disease progression.

2. Materials and methods

2.1. Animals

Male C57BL/6 J mice (22–25 g body weight) were obtained from Shanghai SLAK Laboratory Animal Co., Ltd. and housed under controlled conditions (temperature 25℃, 12/12 h dark/light cycle) with access to food and water ad libitum. All efforts were made to minimize animal suffering. All protocols were approved by the Institutional Animal Care and Use Committee of Huashan Hospital, Fudan University, Shanghai, China and were conducted in accordance with the guidelines and regulations of National Natural Science Foundation of China animal research.

2.2. Surgery

Mice were anesthetized with 5% isoflurane (RWD Life Science, China) for induction and maintained with continuous inhalational 3% isoflurane during surgical operations. Stereotaxic device (RWD Life Science, China) was used for all mice to undergo electrode implantation surgery. 16 mice were assigned to the PTZ model and recovered for 1 week after surgery. Other mice were randomly assigned to receive KA (n = 36) or saline (n = 8) via intrahippocampal injection.

A 5-μl microsyringe was stereotaxically implanted into the right dorsal hippocampal area at the following coordinates for intrahippocampal injections: AP = −2 mm, ML = −1.8 mm, and DV = −2 mm. KA (2 μl; Sigma, Germany) was dissolved in a saline solution at a concentration of 0.1 mg/ml and was injected over 1 min. The needle was maintained in situ for an additional 5 min to avoid reflux along the injection track (Jang et al., 2016). Sham surgery mice were injected with 2 μl of saline. Two electrodes were attached to a microconnector and implanted into skull for EEG recordings at the following coordinates: AP =1.4 mm, ML = −1.8 mm for the recording electrode and AP = −1.5 mm, ML =1.5 mm for the reference electrode (Streijger et al., 2010). The electrodes were covered with a smooth layer of dental acrylic cement.

2.3. EEG and behavior recordings in the PTZ model

On the day of experiments, mice were placed in a 40 × 30 × 50 cm transparent plastic cage and adapted for 30 min. They were randomly divided into the following groups: group I, the mice received tenidap (Tocris, UK) + PTZ (Sigma, Germany) (n = 8); and group II, the mice received DMSO (Sigma, US) + PTZ (n = 8). The dose of tenidap (16 mg/kg) was set according to previous studies and pilot experiments (data not shown). Prior to use, tenidap was dissolved in DMSO at a concentration of 32 mg/ml in a stock solution and diluted with saline to produce the experimental solution at 1.6 mg/ml. Vehicle-control mice received 5% DMSO in a volume of 10 ml/kg of body weight. Baseline video-EEGs were recorded for 30 min prior to tenidap or DMSO administration. Mice were monitored for another 30 min, and PTZ was dissolved with 0.9% saline and administered at dose of 50 mg/kg. All above-mentioned drugs were administered intraperitoneally. Video-EEG monitoring was performed for another 1 h.

EEG signals were captured at a sampling rate of 2500 Hz, amplified 1000 times and filtered from 0.3 to 1000 Hz by using the NeuroLog Electrophysiological Recording System (Digitimer Ltd., UK) and recorded by SPIKE2 software (Cambridge, UK).

2.4. Evaluation of Kir2.3 opening effects in chronically epileptic mice

KA-injected mice (n = 36) were video-EEG monitored directly after surgery for 3 h to verify nonconvulsive status epilepticus (SE), and all mice that survived (n = 31) were terminated with diazepam (5 mg/kg). Mice that exhibited electrographic SE (n = 25) were selected for further experiments. Electrographic SE was defined by the presentation of epileptiform discharges on EEG for more than 2 h (Beamer et al., 2012).

Video-EEG monitoring was performed two weeks after SE (at least 5 h × 7 days) to screen for mice that entered the chronic stage. Detection of at least one spontaneous seizure (SRS) or interictal spiking activity was used as the criterion for chronic stage. 16 mice met the criterion and were used for further study. Tenidap was administered at 16 mg/kg for 7 consecutive days at a regular time (1:00 p.m.) to 6 of the 16 mice so that each animal was used as its own control. Vehicle was injected for comparison in 6 mice. The remaining 4 mice without intervention were used to evaluate possible toxic effects. All 16 mice underwent video-EEG monitoring for another 7 days during this process. The entire procedure is schematically presented in Fig. 4A.

2.5. Seizure measurement

Racine's scale was used to score behavioral epileptic activities in the acute and chronic models, and the onset time was recorded. Briefly, stage I: facial twitching; stage II: head nodding and myoclonic jerks; stage III: unilateral forelimb clonus; stage IV: bilateral forelimb clonus or turning to a side position; and stage V: rearing and falling (loss of postural control) and generalized tonic-clonic seizures (GTCS) (Racine, 1972). We defined clonic seizures (CS) as Racine IV or V epileptic activities.

Quantitative time-frequency power spectrum analysis was performed for EEG traces using MATLAB 2018b (Mathworks, USA) in the PTZ model. Epileptiform spikes with a duration < 100 ms and exceeding twice the baseline amplitude (Chen et al., 2011) were counted manually and using the peak analysis function of Spike2 software in the acute PTZ-induced seizure model and chronic stage of the KA model.

2.6. Immunohistochemistry

16 mice that received PTZ administration as well as 8 normal mice were sacrificed to detect the expression level of c-fos. Mice were anaesthetized with 1% phenobarbital (Sigma, USA) 60 min after PTZ injection and perfused with 0.01 M phosphate buffer (PBS) followed by 4% ice-cold paraformaldehyde (PFA, Sigma, USA). Brains were removed, postfixed in 4% PFA for at least 6 h, progressively immersed in 10% and 30% sucrose over two consecutive days and embedded in OCT. Cryosections were prepared at 30 μm in coronal planes and stored in a cryoprotectant solution at -20℃. Sections of the dorsal hippocampus, assigned to levels from -1.4 to -2.0 mm from bregma were used in subsequent experiments. At the beginning of the experiment, sections were first rinsed 3 times in PBS and mounted on gelatin-coated slides. Sections were blocked in 0.01 M PBS containing 10% donkey serum and 0.3% Triton X-100 at room temperature for 90 min. All slides were incubated with a rabbit anti-c-fos antibody (diluted at 1:500, Santa

Cruz, USA) and a guinea pig anti-NeuN antibody (diluted at 1:800, Abcam, USA) in PBS containing 10% donkey serum at 4℃ overnight. All slides were rinsed 3 times in PBS and incubated with a goat anti-rabbit secondary antibody conjugated to Alexa Fluor 594 and a goat anti-guinea pig secondary antibody conjugated to Alexa Fluor 488 (Molecular Probes, US) at a dilution of 1:500 at room temperature for 2 h in the dark. Slides were rinsed and coverslipped with ProLong Gold antifade reagent (Molecular Probes, USA).

Neuronal morphological alterations of the 16 KA-injected mice with different treatments in the chronic stage and the 8 sham surgery mice were assessed by Nissl staining 28 days after intrahippocampal injection. Brains were obtained and fixed as mentioned above. Coronal sections at the level of dorsal hippocampus were prepared at 10 μm and stained with cresyl fast violet (Beyotime, China).

Immunofluorescent images were captured by a digital microscope (Olympus, Japan) equipped with Cellsens Entry software (Olympus, Japan) and Nissl-stained sections were examined under a bright-field mode. To minimize experimental variability, brains from each group were processed in parallel and imaged under identical settings. For each slice, Neun signal was taken following an exposure of 100 ms, and c-fos signal in exactly the same position was taken with an exposure time of 200 ms. C-fos-positive and Nissl-stained cell were automatically counted using ImageJ Pro (National Institutes of Health, USA) under the 10x objective magnification. The same threshold was set for measuring a certain labeling intensity and were excluded manually. Every fourth consecutively resected brain slices with DG areas defined in 240 × 750 μm fields were used for data analysis, and the number of positive neurons each group was obtained by averaging the mean value of at least four predefined areas of each mouse. Measurements of granule cell layer widths were taken from the hilar border of the granule cell layer (GCL) to the outer borderline of the most distal granule cell somata in the middle of the upper blade of the GCL, and the mean width calculated from selected slices mentioned above was to determine the extent of granule cell dispersion for each animal (Bechstein et al., 2012).

2.7. Statistical analysis

All data are expressed as the means ± SEM. For comparisons between two groups, Student's *t*-test was used for parametric statistics and the Mann-Whitney *U* test was used for nonparametric data. For comparisons between multiple groups, one-way ANOVA and Tukey's multiple comparison test was performed. Categorical variables were analyzed with Fisher's exact test. For statistical analysis of mice before and after tenidap treatment, paired *t*-test was performed. Prism 6.0 (GraphPad Prism Software, USA) was used for all statistical analyses. Values of $p < 0.05$ were considered the threshold for statistical significance.

3. Results

3.1. Pretreatment with tenidap attenuated behavioral and electrographic seizures in PTZ-induced seizure model

As described above, acute seizure represents a brief episode of symptoms due to abnormal neuronal activities. PTZ-induced acute seizures show great practicality and close correlation between behaviors and EEG signals without the subsequent occurrence of SRSs, which makes PTZ a perfect acute convulsant (VelíŠEk, 2006).

To test the anticonvulsant effect of the Kir2.3 agonist tenidap, the latency and duration of CS and GTCS occurrence rate were calculated. The latency of CS failed to reveal statistical significance ($p > 0.05$, Fig. 1A). However, the duration of CS prominently decreased in the mice pretreated with tenidap (425.1 ± 109.9 s) compared to the mice pretreated with DMSO (1727 ± 302.9 s, $p < 0.05$, Fig. 1B). All 8 mice in the DMSO-pretreated group manifested GTCS, and only half of the mice (4 in 8) reached this stage after tenidap pretreatment ($p < 0.05$, Fig. 1C).

PTZ administration elicited repeated high-amplitude spikes on EEGs. Highly synchronized cluster firings were present when Racine V seizures occurred (VelíŠEk, 2006) (Fig. 2A). Tenidap significantly reduced the frequency and amplitude of epileptiform discharges (Fig. 2B). Time-frequency power spectrum analysis showed that the dominant EEG pattern of the tenidap-pretreated mice was 3–5 Hz spikes that were lower than those in the DMSO-pretreated mice with a frequency of 3–10 Hz (Fig. 2C). The intensity of high-frequency firings peaked when GTCS occurred, and the tenidap-pretreated mice without GTCS did not exhibit this pattern. We quantified and averaged the spike frequency on EEG, and the results suggested that tenidap pretreatment significantly decreased the number of spikes (34.71 ± 4.30/min) compared to DMSO pretreatment (65.70 ± 4.32/min, $p < 0.001$, Fig. 2D).

3.2. Tenidap pretreatment decreased c-fos expression in the dentate gyrus of PTZ-induced seizure model mice

C-fos is a frequently used biological marker to evaluate neuronal activation after PTZ-induced acute seizures. As previously described, c-fos first appeared in the Dentate Gyrus (DG) after PTZ injection and peaked 1 h later, but c-fos induction in other hippocampal regions occurred much later (Kiessling and Gass, 1993). Therefore, we performed immunofluorescence assays and compared the number of c-fos-positive neurons in the DG among three groups to reveal the most distinct changes at this time point. There were very few c-fos-positive neurons in the normal control group (13.44 ± 2.86, Fig. 3C, F). Mice that received DMSO pretreatment and developed GTCS after PTZ injection showed enhanced populations of c-fos-positive neurons (99.33 ± 21.40, $p < 0.001$ vs. normal control group, Fig. 3A, D). Tenidap significantly downregulated the number of c-fos-positive neurons in the same area (30.67 ± 3.92, $p < 0.01$ vs. DMSO + PTZ group, Fig. 3B, E), and revealed no significant statistical difference from normal control group. The development of GTCS did not affect the number of c-fos-positive neurons in the tenidap-intervention group.

3.3. Activation of Kir2.3 reversed SRS frequency and abnormal EEG activities in the KA-induced TLE model

Generally, intrahippocampal KA injection elicits nonconvulsive SE with mild convulsions in the acute phase, which means that this model is not the most suitable one to demonstrate the characteristics of a single attack. However, the high survival rate, great reliability and typical morphological alterations in the chronic stage make this model a well-validated model of TLE (Jefferys et al., 2016).

All of the SRSs observed in the 16 KA-induced chronic epileptic mice were associated with epileptiform spikes in EEG, and several interictal EEG discharges without abnormal behavioral manifestations were also recorded (Fig. 4B).In our preliminary experiment, 7-day treatment of tenidap or DMSO exhibited no toxicity for mice. Mice that received sham surgery exhibited neither behavioral seizures nor paroxysmal EEG alterations (Fig. 4C, D), so they were not included into the multiple comparisons. No difference was found regarding neither seizure numbers nor spike numbers between mice with DMSO and mice without intervention (Fig. 4C, D). Tenidap treatment, however, significantly decreased the mean seizure frequency per mouse ($p < 0.01$ vs. KA + DMSO group, $p < 0.01$ vs. KA group) and mean spike frequency per mouse ($p < 0.01$ vs. KA + DMSO group, $p < 0.05$ vs. KA group). Paired comparisons regarding behavioral and electrophysiologic properties of the same mouse before and after tenidap treatment were used to evaluate the therapeutic effect of opening up Kir2.3.The number of seizures before treatment was 4.851 ± 0.6063/h, and decreased significantly to 1.890 ± 0.3646/h ($p < 0.05$, Fig. 4C) after the 7-day intervention with tenidap. The spike frequency on EEG averaged 22.07 ± 8.111/min, and activating the Kir2.3

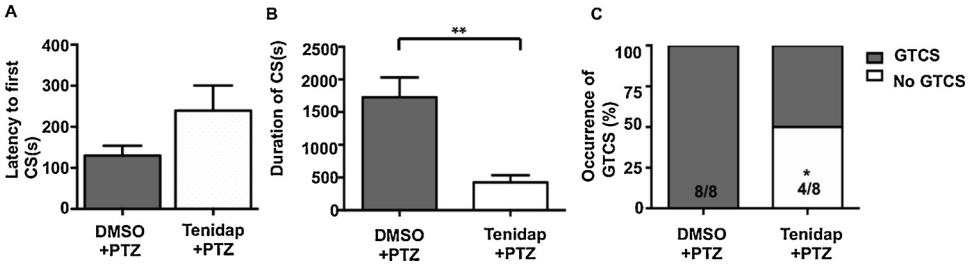

Fig. 1. Activation of Kir2.3 channels suppressed PTZ-induced seizures in mice.
(A) Latency to first CS and (B) duration of CS. Data are presented as mean ± SEM for n = 8 per group. (C)The occurrence of GTCS in two groups with or without tenidap pretreatment (n = 8, respectively). *$p < 0.05$ compared with DMSO + PTZ group; **$p < 0.01$ compared with DMSO + PTZ group. Statistically significant differences in (A), (B) were determined using unpaired student's *t*-test. Statistically significant differences in (C) was determined using Fisher's exact test.

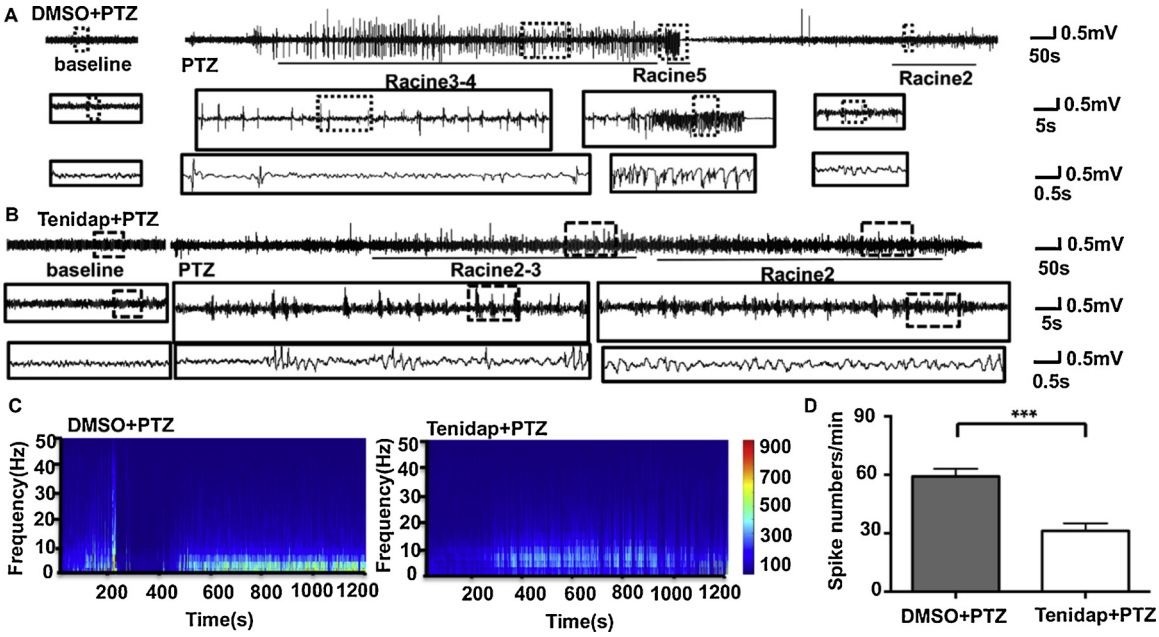

Fig. 2. Representative EEG traces with their time-frequency power heat plots and spike numbers demonstrating the effect of tenidap on PTZ-treated mice.
(A–B) EEG traces recorded from skull-electrodes of DMSO + PTZ group (A) and tenidap + PTZ group (B) starting from the administration of PTZ and lasting for 20 min. The traces in the dashbox are enlarged under their original ones to show the details. (C) Time-frequency power heat plots to show above EEG signals received DMSO or tenidap pretreatment. (D) The effect of tenidap pretreatment on EEG spike numbers. *** $p < 0.001$ compared with DMSO + PTZ group. Statistically significant differences in (D) was determined using unpaired student's *t*-test.

channel attenuated the epileptiform discharges to 1.748 ± 0.7328/min ($p < 0.05$, Fig. 4D). The percentage of maximal Racine score was used to evaluate seizure severity. Racine V episodes dominated before tenidap administration, but these episodes were completely abolished at the beginning of the therapeutic process. Racine III-IV seizures became the maximal response after Kir2.3 activation (Fig. 4G).

3.4. Successive administration of tenidap decreased neuronal loss in the hippocampus of KA-induced TLE model mice

Nissl staining was performed to detect the two main morphological features of the TLE model, namely, hilar neuronal loss and granule cell dispersion (GCD) (Buckmaster and Dudek, 1997). Nissl-stained sections of sham surgery mice exhibited regularly scattered neurons in the hilus (414.90 ± 38.70, Fig. 5A) and extensive neurons in the GCL of Dentate Gyrus (width of GCL, 99.40 ± 3.52 μm, Fig. 5A), which demonstrated that there was no neuronal damage in this group. KA-induced epileptic mice showed severe hilar neuronal loss (95.60 ± 16.55, Fig. 5D, $p < 0.001$ vs. sham surgery mice, Fig. 5E) and scattered GCL (146.00 ± 6.88, Fig. 5D, $p < 0.05$ vs. sham surgery mice, Fig. 5F). The KA-injected mice with DMSO showed a marked degree of GCL widening (148.40 ± 12.53 μm, Fig. 5C, $p < 0.01$ vs. sham surgery mice, Fig. 5F) and significant neuronal loss in the hilus (102.30 ± 13.10, Fig. 5C, $p < 0.001$ vs. sham surgery mice, Fig. 5E) ipsilateral to the injection site. Mice treated with tenidap also suffered hippocampal injuries (217.80 ± 15.97 neurons in the hilus, Fig. 5B, $p < 0.001$ vs. sham surgery mice, Fig. 5E) but showed protection in hilar neuronal loss than DMSO-control mice ($p < 0.05$ vs. KA + DMSO mice, $p < 0.05$ vs. KA mice, Fig. 5E). Widening of GCL remained significant after 7-day administration of tenidap (139.4 ± 11.61 μm, Fig. 5B, $p < 0.05$ vs. sham surgery mice, Fig. 5F). The treatment tended to decrease the extent of dispersion, but failed to reveal differences when compared with other KA-induced epileptic mice ($p > 0.05$ vs. KA + DMSO mice, $p > 0.05$ vs. KA mice, Fig. 5F). The morphological changes in all the KA-injected mice were restricted to the ipsilateral hippocampus.

4. Discussion

Kir2.3 exhibits a characteristic property of strong inward rectification that regulates the resting membrane potential and firing threshold in neurons (Neusch et al., 2003). We detected protein expression in a rat pilocarpine model, which suggested that activation of Kir2.3 exerted a counterbalancing role in the acute phase and whereas downregulation of it may facilitate the occurrence of spontaneous seizures (Xu et al., 2013). The potential relationship between Kir2.3 and epilepsy directed our efforts to identify and develop putative antiepileptic agents targeting Kir2.3. However, the antiepileptic effects of Kir2.3 activation

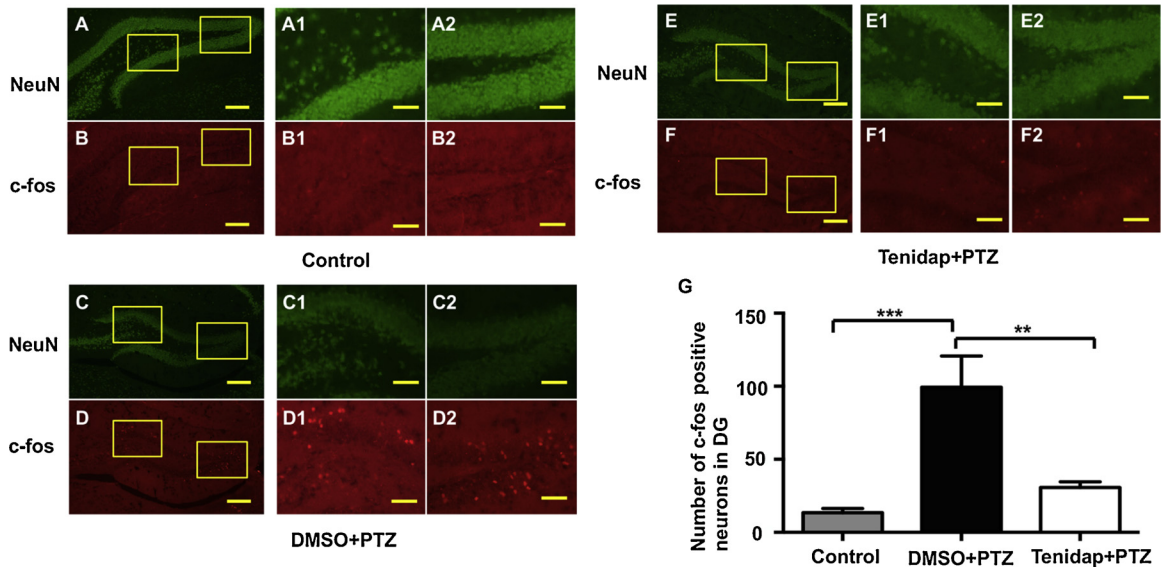

Fig. 3. Activation of Kir2.3 suppresed c-fos expression in DG area.
(A–F) Immunoreactivity of NeuN and c-fos in the DG area of normal control mice (A–B), mice pretreated with DMSO (C–D) or tenidap (E–F) at 1 h after PTZ injection. The rectangled areas in (A—F) are further enlarged in numbered panels on their right sides, respectively. (G) The effect of tenidap on number of c-fos positive neurons in DG. $^{**}p < 0.01$, $^{***}p < 0.001$ compared with DMSO + PTZ group. Scale bar indicates 100 μm in "A-F" and 25 μm in "A1-F1,A2-F2". Statistically significant differences in (G) was determined using one-way ANOVA and Tukey's multiple comparison test.

need further attention and new evidence in a direct way, especially during the chronic TLE stage. The present study demonstrated that the specific Kir2.3 agonist tenidap attenuated seizure activities and neuronal excitability in the PTZ acute model. For chronic KA model, activating Kir2.3 decreased SRS frequency and impeded hilar neuronal loss.

Our current work investigated Kir2.3 as the potential antiepileptic target. First, we used two seizure models tailored to different research demands. The acute convulsant PTZ induces a wide spectrum of epileptic activities in a relatively short time and results in only transient neuronal injury. A chronic epileptic model requires the presence of SE characterized by continuous seizure activities, which represent the initial precipitating assault that will lead to a subsequent epileptogenesis and the occurrence of SRSs. Both pilocarpine and KA chronic models exhibit these characteristics. KA induces higher SRS frequency than the pilocarpine model, which makes the KA model more advantageous for the detection of subtle changes. The pharmacological response of acute seizures may differ from spontaneous recurrent seizures, but data in the chronic stage of the TLE model were absent in our previous study. Therefore, we used the KA-induced chronic epileptic model to provide more information of therapeutic value. We showed that activation of Kir2.3 decreased the duration and the maximal response of seizures in the PTZ model and remarkably lowered SRS frequency in the KA model, which reinforced the anticonvulsant and disease-modifying effects of activating this channel. No significant differences in the latencies of

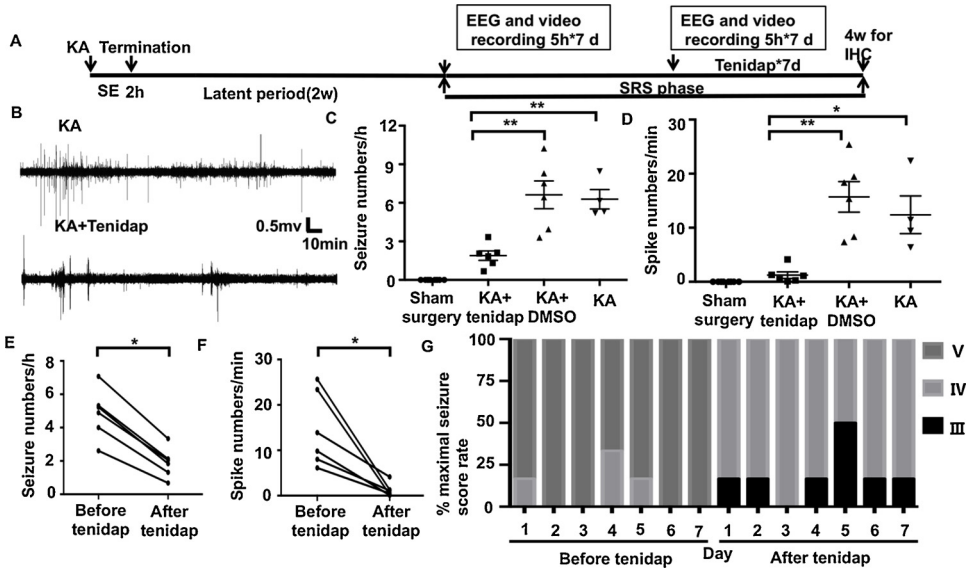

Fig. 4. Scheme of experimental design for video-EEG recording and the disease-modifying effect of tenidap administration in KA chronic epileptic model.
(A) After the establishment of SE, we waited for 2 weeks and started video-EEG recording to determine whether they entered the chronic phase and learn about their basic levels in SRS frequency. Then tenidap was administered daily with video-EEG monitoring for another 7 days. All mice were sacrificed on 28th day for Nissl staining. (B) Representative EEG traces demonstrating one of the KA-induced epileptic mice in its recording sessions during SRS phase before and after tenidap treatment respectively. (C–D) Multiple comparisons of KA-induced epileptic mice with different treatment. Average of SRS numbers per hour (C) and average of spike frequency (D) during 7-day recordings were analyzed. Every point represents the average of seizure frequency or spike frequency for an individual animal; $^{*}p < 0.05$, $^{**}p < 0.01$ compared with the KA + tenidap group. (E–F) The effect of tenidap in KA-induced chronic epileptic mice. Mean seizure numbers per hour (E) and mean spike numbers per minute (F) before and after the intervention of tenidap during the 7-day recording period. Black points represent the average of seizure frequency or spike frequency for an individual animal; black lines connecting dots indicate the same animal. $^{*}p < 0.05$ compared with the same mice before tenidap treatment. (G) Proportion of mice with their highest seizure score on each day. Statistically significant differences in (C), (D) were determined using one-way ANOVA and Tukey's multiple comparison test. Statistically significant differences in (E), (F) were determined using paired *t*-test.

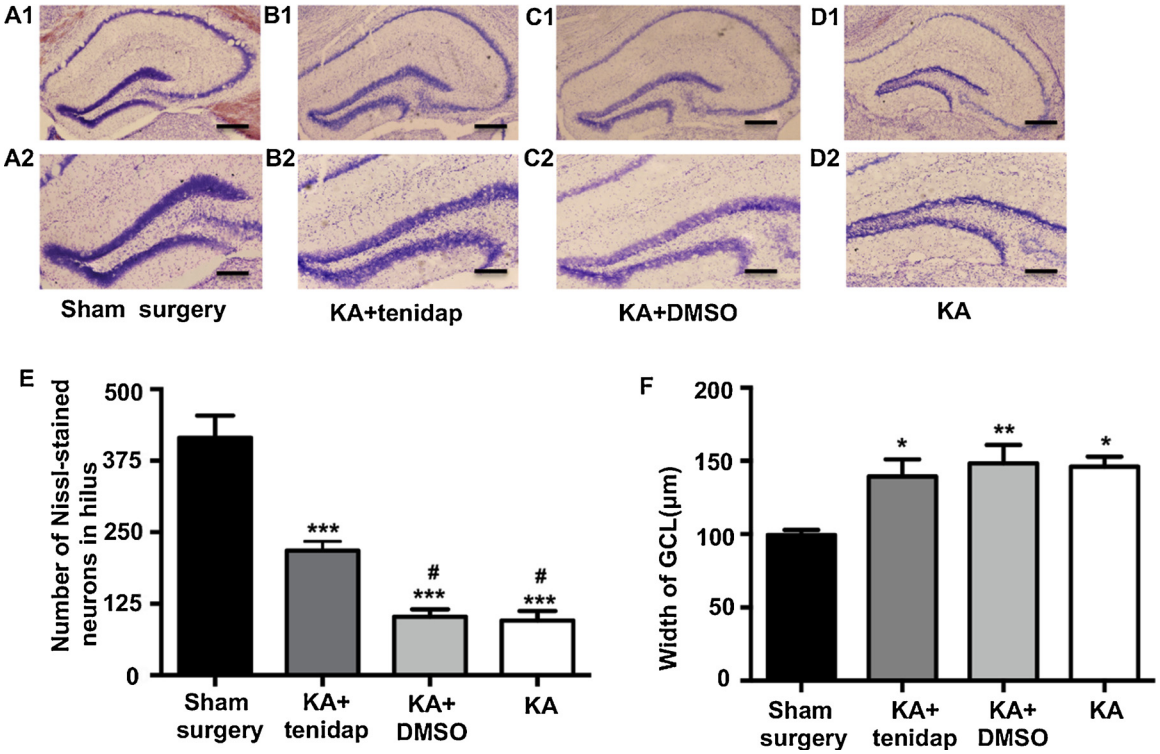

Fig. 5. Tenidap reduced hippocampal neuron loss in KA-induced chronic epileptic model.
(A–D) Representative Nissl-stained hippocampal sections of sham surgery (A), KA + tenidap (B), KA + DMSO (C) and KA without intervention (D) groups on 28 days after surgery. Magnification images of the hilus and Dentate Gyrus are shown below panel A1-D1 respectively. (E) Measurement of Nissl-stained neurons in hilus among 4 groups. (F) Histogram showing the granule cell layer width among 4 groups.
$^{*}p < 0.05$, $^{**}p < 0.01$, $^{***}p < 0.001$ compared with sham surgery group. $\#p < 0.05$ compared with KA + tenidap group. Scale bar indicates 200μm in A1-D1 and 100μm in A2-D2. Statistically significant differences in (E), (F) were determined using one-way ANOVA and Tukey's multiple comparison test.

seizure onset in PTZ model may indicate that Kir2.3 opening inhibits the propagation of excitability rather than producing a direct anti-epileptogenic effect. The detection of a sensitive biomarker in the PTZ model was designed to test the activation level of neurons, and classic Nissl staining was used in the KA model to further evaluate cytoarchitectural alterations.

The basal expression level of c-fos in hippocampal neurons is relatively low. Triggering expression of c-fos presumably participates in the molecular cascades involving seizure generation, and the highest activation level in PTZ-induced acute seizures occurred in the DG, as previously reported (Herrera and Robertson, 1996). The remarkable suppression of c-fos induced by Kir2.3 activation indicated reduced cellular excitability associated with the inhibition of acute-induced seizures. Notably, the immunoactivity of c-fos changed drastically in the GCL in our present study. Normally, the GCL serves as a gate to prevent excessive synchronicity into the hippocampus and protects granule cells from activation. Breakdown of the GCL with granule cell hyperexcitability is considered a critical event in the development of temporal lobe seizures, and periodic disruption of this filtering gate may lead to SRS (Krook-Magnuson et al., 2015). Therefore, the especially down-regulated c-fos-positive neurons in the GCL suggesting decreased hyperexcitability may also be beneficial for the suppression of epileptogenesis of TLE. We did not study c-fos levels in the SRS stage because too many confounding factors existed, and it is too difficult to handle the interval time between SRSs.

Previous reports suggested that reduced Kir channel expression lead to disturbed K^+ buffering and enhanced seizure susceptibility in a chronic TLE model (Djukic et al., 2007). Administration of the specific Kir2.3 opener tenidap, which was also developed as an anti-inflammatory agent, demonstrated a significant disease-modifying effect by reducing SRS and spike frequency after the establishment of TLE in our present study. Besides, we further investigated whether tenidap prevents cytoarchitectural changes from recurrent seizures and inflammatory attacks. Although hilar neuronal loss was protected by tenidap, the measurement of GDL width failed to reveal differences between different treatment conditions, which may be attributed to the timing of the intervention. A reduction in the hippocampal excitability was reported to affect GCD in only a few days following KA injection, which means that a reorganization of neuronal circuits already completed during the latent period before our intervention (Riban et al., 2002; Antonucci et al., 2008). However, neuronal death does not necessarily progress in parallel with GCD, and the degeneration that is initiated after SE may evolve over a longer time. Therefore, recurrent seizures may gradually exacerbate the situation (Zhang et al., 2002; Suzuki et al., 2005). Our results demonstrated that 7-day tenidap treatment significantly protected mice from hippocampal (at least hilar neurons) injuries.

We are aware that a number of caveats exist in the present study. The role of Kir2.3 in epileptogenesis is not clear, and the phase-to-disease onset represents a crucial period of time to investigate the mechanisms involved. Whether the effect of tenidap on neuronal protection resulted from reduced SRS frequency per se or in cooperation with anti-inflammatory mechanisms requires further investigation. Establishing Kir2.3 knockdown mice would be used in our future research to draw a definitive conclusion.

5. Conclusion

The present study demonstrated the anticonvulsant properties of Kir2.3 activation in acute PTZ and chronic KA models in adult mice. The expression levels of c-fos in acute seizures confirmed that Kir2.3 activation reduced neuronal excitability. Seven days of tenidap

administration significantly abrogated neuronal loss. These results support Kir2.3 as a promising target for epilepsy modulation.

Declaration of Competing Interest

The authors declare no conflicts of interest.

Acknowledgment

This work was supported by a grant from the National Natural Science Foundation of China (grant number 81671280).

References

Antonucci, F., Di Garbo, A., Novelli, E., Manno, I., Sartucci, F., Bozzi, Y., Caleo, M., 2008. Botulinum neurotoxin E (BoNT/E) reduces CA1 neuron loss and granule cell dispersion, with no effects on chronic seizures, in a mouse model of temporal lobe epilepsy. Exp. Neurol. 210, 388–401.

Beamer, E., Otahal, J., Sills, G.J., Thippeswamy, T., 2012. N (w) -propyl-L-arginine (L-NPA) reduces status epilepticus and early epileptogenic events in a mouse model of epilepsy: behavioural, EEG and immunohistochemical analyses. Eur. J. Neurosci. 36, 3194–3203.

Bechstein, M., Haussler, U., Neef, M., Hofmann, H.D., Kirsch, M., Haas, C.A., 2012. CNTF-mediated preactivation of astrocytes attenuates neuronal damage and epileptiform activity in experimental epilepsy. Exp. Neurol. 236, 141–150.

Buckmaster, P.S., Dudek, F.E., 1997. Neuron loss, granule cell axon reorganization, and functional changes in the dentate gyrus of epileptic kainate-treated rats. J. Comp. Neurol. 385, 385–404.

Chen, C.R., Tan, R., Qu, W.M., Wu, Z., Wang, Y., Urade, Y., Huang, Z.L., 2011. Magnolol, a major bioactive constituent of the bark of Magnolia officinalis, exerts antiepileptic effects via the GABA/benzodiazepine receptor complex in mice. Br. J. Pharmacol. 164, 1534–1546.

Das, A., Wallace, G.Ct, Holmes, C., McDowell, M.L., Smith, J.A., Marshall, J.D., Bonilha, L., Edwards, J.C., Glazier, S.S., Ray, S.K., Banik, N.L., 2012. Hippocampal tissue of patients with refractory temporal lobe epilepsy is associated with astrocyte activation, inflammation, and altered expression of channels and receptors. Neuroscience 220, 237–246.

Djukic, B., Casper, K.B., Philpot, B.D., Chin, L.S., McCarthy, K.D., 2007. Conditional knock-out of Kir4.1 leads to glial membrane depolarization, inhibition of potassium and glutamate uptake, and enhanced short-term synaptic potentiation. J. Neurosci. 27, 11354–11365.

Greene, D.L., Hoshi, N., 2017. Modulation of Kv7 channels and excitability in the brain. Cell. Mol. Life Sci. 74, 495–508.

Gunthorpe, M.J., Large, C.H., Sankar, R., 2012. The mechanism of action of retigabine (ezogabine), a first-in-class K+ channel opener for the treatment of epilepsy. Epilepsia 53, 412–424.

Herrera, D.G., Robertson, H.A., 1996. Activation of c-fos in the brain. Prog. Neurobiol. 50, 83–107.

Hibino, H., Inanobe, A., Furutani, K., Murakami, S., Findlay, I., Kurachi, Y., 2010. Inwardly rectifying potassium channels: their structure, function, and physiological roles. Physiol. Rev. 90, 291–366.

Jang, H., Jeong, K.H., Kim, S.R., 2016. Naringin attenuates granule cell dispersion in the dentate gyrus in a mouse model of temporal lobe epilepsy. Epilepsy Res. 123, 6–10.

Jefferys, J., Steinhauser, C., Bedner, P., 2016. Chemically-induced TLE models: topical application. J. Neurosci. Methods 260, 53–61.

Kambli, L., Bhatt, L.K., Oza, M., Prabhavalkar, K., 2017. Novel therapeutic targets for epilepsy intervention. Seizure 51, 27–34.

Kiessling, M., Gass, P., 1993. Immediate early gene expression in experimental epilepsy. Brain Pathol. 3, 381–393.

Krook-Magnuson, E., Armstrong, C., Bui, A., Lew, S., Oijala, M., Soltesz, I., 2015. In vivo evaluation of the dentate gate theory in epilepsy. J. Physiol. 593, 2379–2388.

Liu, Y., Liu, D., Printzenhoff, D., Coghlan, M.J., Harris, R., Krafte, D.S., 2002. Tenidap, a novel anti-inflammatory agent, is an opener of the inwardly rectifying K+ channel hKir2.3. Eur. J. Pharmacol. 435, 153–160.

Neusch, C., Weishaupt, J.H., Bahr, M., 2003. Kir channels in the CNS: emerging new roles and implications for neurological diseases. Cell Tissue Res. 311, 131–138.

Racine, R.J., 1972. Modification of seizure activity by electrical stimulation. II. Motor seizure. Electroencephalogr. Clin. Neurophysiol. 32, 281–294.

Riban, V., Bouilleret, V., Pham-Le, B.T., Fritschy, J.M., Marescaux, C., Depaulis, A., 2002. Evolution of hippocampal epileptic activity during the development of hippocampal sclerosis in a mouse model of temporal lobe epilepsy. Neuroscience 112, 101–111.

Rogawski, M.A., Loscher, W., 2004. The neurobiology of antiepileptic drugs. Nat. Rev. Neurosci. 5, 553–564.

Streijger, F., Scheenen, W.J., van Luijtelaar, G., Oerlemans, F., Wieringa, B., Van der Zee, C.E., 2010. Complete brain-type creatine kinase deficiency in mice blocks seizure activity and affects intracellular calcium kinetics. Epilepsia 51, 79–88.

Suzuki, F., Heinrich, C., Boehrer, A., Mitsuya, K., Kurokawa, K., Matsuda, M., Depaulis, A., 2005. Glutamate receptor antagonists and benzodiazepine inhibit the progression of granule cell dispersion in a mouse model of mesial temporal lobe epilepsy. Epilepsia 46, 193–202.

VelÍŠEk, L., 2006. CHAPTER 11 - Models of chemically-induced acute seizures. In: Pitkänen, A., Schwartzkroin, P.A., Moshé, S.L. (Eds.), Models of Seizures and Epilepsy. Academic Press, Burlington, pp. 127–152.

Xu, L., Hao, Y., Wu, X., Yu, P., Zhu, G., Hong, Z., 2013. Tenidap, an agonist of the inwardly rectifying K+ channel Kir2.3, delays the onset of cortical epileptiform activity in a model of chronic temporal lobe epilepsy. Neurol. Res. 35, 561–567.

Young, C.C., Stegen, M., Bernard, R., Müller, M., Bischofberger, J., Veh, R.W., Haas, C.A., Wolfart, J., 2009. Upregulation of inward rectifier K+ (Kir2) channels in dentate gyrus granule cells in temporal lobe epilepsy. J. Physiol. 587, 4213–4233.

Zhang, X., Cui, S.S., Wallace, A.E., Hannesson, D.K., Schmued, L.C., Saucier, D.M., Honer, W.G., Corcoran, M.E., 2002. Relations between brain pathology and temporal lobe epilepsy. J. Neurosci. 22, 6052–6061.